Hindawi
Journal of Control Science and Engineering
Volume 2022, Article ID 8962970, 12 pages
https://doi.org/10.1155/2022/8962970

Research Article

Swarm Control for Multiple Unmanned Surface Vehicles with Unknown Time-Varying Environmental Disturbance and Input Saturation

Guoqing Xia and Xianxin Sun

College of Intelligent Systems Science and Engineering, Harbin Engineering University, Harbin 150001, China

Correspondence should be addressed to Xianxin Sun; hrbsunxianxin@hrbeu.edu.cn

Received 2 March 2022; Revised 5 June 2022; Accepted 14 June 2022; Published 11 July 2022

Academic Editor: Petko Petkov

This paper addresses the swarm tracking problem of multiple unmanned surface vehicles subjected to unknown time-varying environmental disturbance and input saturation. The main control objective of this paper is that USVs cluster to follow the virtual leader with the desired position and heading and are required to maintain a specified position separation relative to both neighbor vehicles. In order to achieve the design goal, we mainly focus on three aspects. Firstly, to estimate the external disturbance accurately and improve the convergence speed, a finite-time disturbance observer is designed. Secondly, an auxiliary dynamic system is introduced to solve the input saturation problem. Thirdly, an output feedback controller based on a finite-time disturbance observer and an auxiliary dynamic system is designed to achieve swarm control of multiple unmanned surface vehicles. The stability of the system is proved by the Lyapunov directly method. Finally, the simulation results show that the proposed control strategy is effective.

1. Introduction

In recent years, swarm control for multiple unmanned surface vehicles (USVs) has attracted increasing interest in many fields, such as search and track mission [1], rescue operations [2], and dynamic guarding [3, 4]. These have brought new challenges to USV cluster control, especially maintaining a desired position separation relative to what is often required when USVs swarm to perform the corresponding missions [5].

These challenges can be divided into two aspects: unknown time-varying environmental disturbance and input saturation. The environmental disturbance is caused by the wind, waves, and ocean currents in surge, sway, and yaw, respectively. Due to the environmental disturbance being unknown and time-varying, it cannot be measured directly and accurately. Therefore, some control strategies based on estimating disturbance or compensating for disturbance are proposed in [6–11]. Through these proposed control strategies, the observation error only accurately estimates rather than converges to a small neighborhood of an equilibrium state as soon as possible. Furthermore, to improve the convergence speed, the finite-time control technology is adopted in [12–16], which ensures the consistency of all states in the closed-loop system in a finite time. Therefore, the combination of disturbance observer and finite-time control technology is an executable program.

Except for environmental disturbance, another challenge to USVs' cluster control is input saturation. Since the USV actuator cannot be infinite, there is a deviation between the expected input signal and the actual output of the actuator. Therefore, the amplitude of the control signal is usually limited to a certain range. In the process of designing the actuator, it is necessary to consider the physical constraints of the actuator, that is, input saturation. The existence of input saturation may lead to system oscillation and even system instability. In recent years, the input saturation problem of various systems has received the most extensive

attention. In [17], an adaptive mechanism is devised to figure out the input saturation problem. In [18], a novel finite-time control approach is presented to overcome the effects of state constraints on system performance. The group consensus algorithms with input saturation are given in [19]. From the vessels' work situation, it is very necessary to take input saturation into account in cluster control through the actual working conditions of the multiple USVs.

Based on the above research background, for the first challenge, a finite-time disturbance observer is proposed to resolve the first challenge, which can not only measure the disturbance accurately, but also improve the converge speed. Secondly, by using an auxiliary dynamic system to solve the second problem of input saturation. Furthermore, to solve the above two challenges more perfectly, an output feedback controller is proposed, which is mainly composed of a finite time-disturbance observer, an auxiliary dynamic system, and other control technologies. Meanwhile, it is proved that all signals in the closed-loop system are bounded by the Lyapunov method.

The main contributions of this paper are summarized as follows: firstly, different from existing disturbance observer approaches in [20], the unknown time-varying environmental disturbance can be measured accurately by the finite-time disturbance observer. Secondly, unlike the existing work ignoring the actuator constraints, an auxiliary dynamic system is introduced to resolve the input saturation problem. Thirdly, an output feedback controller is designed, which is mainly composed of a finite-time disturbance observer, an auxiliary dynamic system, and other control technologies.

A summary of recent works is outlined in Table 1, corresponding to different features and classification.

This paper is organized as follows: Section 2 describes some necessary preliminaries and mathematical modeling of USVs. Section 3 depicts the finite-time disturbance observer design. Section 4 describes the output feedback controller design and stability analysis. Simulation results and comparison results are discussed in Section 5 and Section 6 concludes this paper.

Notations: the following notations will be used throughout this paper. A/B denotes all elements that belong to A and not to B. $|\cdot|$ represents the absolute value of a scalar. $\|\cdot\|$ denotes the Euclidean norm. $\mathbf{R}^{m\times n}$ represents the $m\times n$ dimensional Euclidean Space. $\mathrm{diag}\{a_i\}$ denotes a block-diagonal matrix with a_i being the ith diagonal element. $(\cdot)^T$ and $(\cdot)^{-1}$ represent the transpose and inverse of a matrix, respectively. $\otimes$ denotes the Kronecker product of matrix. $\lambda_{\min}(\cdot)$ and $\lambda_{\max}(\cdot)$ represent minimum and maximum of eigenvalues a matrix, respectively. $sig^{\delta}(\cdot) = |\cdot|^{\delta}\mathrm{sign}(\cdot)$, sign represents the Symbolic function, i.e., $\mathrm{sign}(t) = -1$, $\forall t < 0$; $\mathrm{sign}(t) = 0$, $t = 0$; $\mathrm{sign}(t) = 1$, $\forall t > 0$. I_n represents the $n\times n$ dimensional identity matrix. i is used to denote the subscript of USVs.

2. Preliminaries and Mathematical Modeling of USVs

2.1. Algebraic Graph Theory. Graph theory is used to describe the communication topology of n follower USVs and a virtual leader vehicle (denoted by 0). A directed graph $\mathcal{G} = (\mathcal{V}, \varepsilon)$ consists of a vertex set $\mathcal{V} = \{0, 1, 2, \ldots, n\}$ and the set of edges $\varepsilon \subseteq \{(i, j) \in \mathcal{V}\times\mathcal{V}\}$. A directed edge (i, j) is not only the incoming edge of node j but also the outgoing edge of node i. If $(i, j) \in \varepsilon$, node j is an adjacent node of node i. The set of all adjacent nodes of node i is represents by $\mathcal{N}_i = \{j \in \mathcal{V}, (i, j) \in \varepsilon\}$, see [21].

Consider a directed graph $\mathcal{G}$ composed of n nodes, the adjacency matrix $\mathcal{A} = [a_{ij}]_{n\times n}$ is used to represent the link relationship between nodes, where $a_{ij} = 1$, if $(i, j) \in \varepsilon$; $a_{ij} = 0$, otherwise. If $a_{ij} = a_{ji}$, the graph is undirected; otherwise is directed. The Laplacian matrix $\mathcal{L}$ associates with the graph $\mathcal{G}$ is defined as $\mathcal{L} = \mathcal{D} - \mathcal{A}$ where $\mathcal{D} = \mathrm{diag}\{d_1, d_2, \ldots, d_n\}$ with $d_i = \sum_{j=1}^{n} a_{ij}$. Laplacian matrix $\mathcal{L}$ always has a right eigenvector of $1_n = (1, 1, \ldots, 1)^T$ associated with eigen value $\lambda_1 = 0$.

In particular, a diagonal matrix $\mathcal{A}_0 = \mathrm{diag}\{a_{i0}\}$ is defined as a leader adjacency matrix, where $a_{i0} = 1$, if and only if the i th USV receives information from the virtual leader vehicle; $a_{i0} = 0$, otherwise. Finally, the information exchange matrix is defined as $\mathcal{H} = \mathcal{L} + \mathcal{A}_0$.

Assump 1. The graph $\mathcal{G}$ is directed, and there is at least one spanning tree from the root node to the leader node, i.e., the $\mathcal{H}$ is a positive definite matrix.

2.2. Finite Time Stability

Lemma 1 (see [13]). *Consider the system of differential equations*

$$\begin{aligned} \dot{y}(t) &= f(y(t)),\\ f(0) &= 0, \end{aligned} \tag{1}$$

where $f: U \longrightarrow R^n$ is continuous on an open neighborhood $U\subseteq\mathbf{R}^n$ of the origin. A continuously differentiable function $y: T \longrightarrow U$ is said to be a solution of formula (1) on the interval $T \subset \mathbf{R}$ if $y(t)$ satisfies formula (1) for all $t \in T$.

Suppose there exists a continuous positive definite function $V: U \longrightarrow \mathbf{R}$, real numbers $c_1 > 0, c_2 \in (0, 1)$ and an open neighborhood $U_0\subseteq U$ of the origin such that

$$\dot{V}(x) + c_1 (V(x))^{c_2} \le 0, \quad x \in U_0\backslash\{0\}. \tag{2}$$

Then the origin is a finite-time-stable equilibrium of (1).

Moreover, if $U = \mathbf{R}^n$, $V(x)$ is proper, and $\dot{V}(x)$ takes negative values on $\mathbf{R}^n\backslash\{0\}$, then the origin is a globally finite-time-stable equilibrium of (1). And T is called the convergence-time function, it satisfies

$$T(x) \le \frac{1}{c_1(1 - c_2)} (V(x))^{1-c_2}, \quad x \in \mathbf{R}^n\backslash\{0\}. \tag{3}$$

2.3. USVs Modeling. Consider a group of USVs swarm consisting a virtual leader vehicle (subscript is 0) and n follower USVs (subscript is $1, 2, \ldots, n$), the 3 degrees of freedom (DOFs) kinematics and dynamics equations of the i th USV can be expressed in vector form as follows:[23]

Table 1: Recent works on consensus problems.

Features	Classification	References
About environmental disturbance	Formation control	[6]
	Tracking control	[7, 8]
	Output-feedback control	[5, 9, 10]
About time control	Fixed-time control	[11]
	Finite-time control	[12–16]
	Time-varying control	[21]
Constraints	Input saturation	[17, 19, 22]
	Full state constraints	[18]

$$\dot{\eta}_i = R_i(\psi_i)\upsilon_i, \tag{4}$$

$$M_i\dot{\upsilon}_i + D_i\upsilon_i = \tau_i + d_i, \tag{5}$$

where $R_i(\psi_i)$ is the rotation matrix, it is given as follows:

$$R_i(\psi_i) = \begin{bmatrix} \cos(\psi_i) & -\sin(\psi_i) & 0 \\ \sin(\psi_i) & \cos(\psi_i) & 0 \\ 0 & 0 & 1 \end{bmatrix}, \tag{6}$$

with properties: $\|R_i(\psi_i)\| = 1$ and $R_i^T R_i(\psi_i) = I_{3\times 3}$. $\eta_i := [x_i, y_i, \psi_i]^T$ is the position and yaw angle in the earth-fixed frame $X_E O_E Y_E$ (see Figure 1). $\upsilon_i := [u_i, v_i, r_i]^T$ is the velocity vector in the body-fixed frame $X_B O_B Y_B$. The system inertia matrix $M_i \in \mathbf{R}^{3\times 3}$ is positive definite and constant, where $M_i = M_i^T$ and $\dot{M}_i = 0$. The damping matrix $D_i \in \mathbf{R}^{3\times 3}$ is also symmetric and positive define. $\tau_i := [\tau_{i1}, \tau_{i2}, \tau_{i3}]^T$ is the control input, which is produced by the propellers. $d_i := [d_{i1}, d_{i2}, d_{i3}]^T$ is unknown time-varying environmental disturbance, which caused by the wind, waves, and ocean currents in surge, sway, and yaw, respectively.

In this paper, considering the input saturation constraint, the control forces and moment produced via the propellers are limited. The input saturation constraint can be described as follows:

$$\tau_i = \begin{cases} \tau_{i,\max}, & \text{if } \tau_{ic} > \tau_{i,\max}, \\ \tau_{ic}, & \text{if } \tau_{i,\min} \le \tau_{ic} \le \tau_{i,\max}, \\ \tau_{i,\min}, & \text{if } \tau_{ic} < \tau_{i,\min}, \end{cases} \tag{7}$$

where $\tau_{i,\max} \in \mathbf{R}^3$ and $\tau_{i,\min} \in \mathbf{R}^3$ are the maximum and minimum control forces and moment of i th vehicle, respectively. $\tau_{ic} = [\tau_{ic1}, \tau_{ic2}, \tau_{ic3}]^T$ is calculated by the output feedback controller.

The main goal of this paper is to design a control law so that the USVs can track the desired reference point while maintaining a fixed formation, i.e.,

$$\lim_{t\longrightarrow+\infty} \|\eta_i - \eta_d - \mu_i\| \le \sigma_i, \tag{8}$$

where $\eta_d := [x_d, y_d, \psi_d]^T$ is the desired reference point. $\mu_i := [x_{i\mu}, y_{i\mu}, \psi_{i\mu}]^T$ represents the expected relative deviation position and heading between the i th USV and the desired reference point. In order to maintain fixed formation

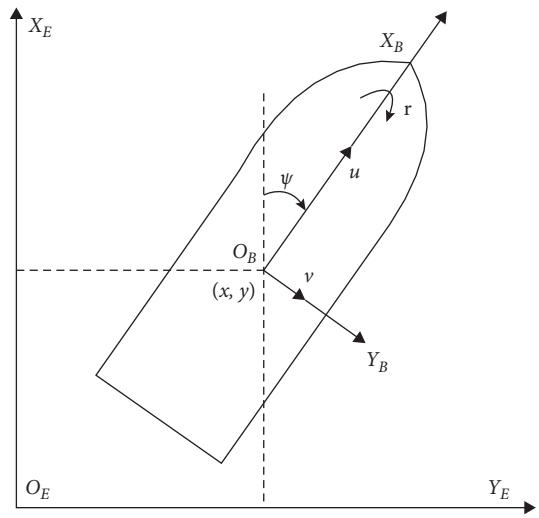

Figure 1: Earth-fixed frame and body-fixed frame.

for USVs cluster, thus μ_i is a constant vector. $\sigma_i > 0$ is a positive constant.

Assump 2. The reference signal η_d is smooth and differentiable everywhere. Its first derivative $\dot{\eta}_d$ and second derivative $\ddot{\eta}_d$ exist and are bounded.

Assump 3. The time-varying environmental disturbances d_i is unknown but bounded, and its first derivative $\dot{d}_i$ exists and is bounded, i.e.,

$$\|d_i\| \le d_{i,\max}, \ \|\dot{d}_i\| \le c_3, \tag{9}$$

where $d_{i,\max} > 0$ and $c_3 > 0$ are positive constants.

Assump 4. The system inertia matrix M_i and damping matrix D_i are known.

2.4. Environmental Disturbances Modeling. . Unmodeled external forces and moment due to wind, ocean currents, and second waves are lumped together into an earth-fixed slowly-varying bias term $d_i \in \mathbf{R}^3$ [24, 25]. A widely used bias model for USVs is the first-order Markov process [26–28]. In this paper, the environmental disturbances are modeled as follows:

$$d_i = -R_i^T b, \tag{10}$$

where b represents the first-order Markov process, it is given as follows:

$$\dot{b} = -\mathrm{T}^{-1} b + \mathrm{E}_b \vartheta_b, \tag{11}$$

where $\mathrm{T} \in \mathbf{R}^{3\times 3}$ is the diagonal matrix of positive bias time constants, $\mathrm{E}_b \in \mathbf{R}^{3\times 3}$ is the diagonal matrix scaling the amplitude of the ϑ_b, $\vartheta_b \in \mathbf{R}^3$ is a vector of zero-mean Gaussian while noise.

3. Finite-Time Disturbance Observer Design

Owing the environmental disturbance is unknown and time-varying, the accurate value is difficult to receive directly. To solve this problem, a finite-time disturbance observer (FTDO) is designed as follows:

$$M_i\dot{\hat{v}}_i = -D_i v_i + \tau_i + \hat{d}_i, \tag{12}$$

where $\hat{d}_i$ is the estimate of the unknown time-varying environmental disturbance d_i, $\hat{v}_i$ is the estimate of v_i.

A new variable is defined as follows:

$$\omega_i = M_i v_i - M_i \hat{v}_i, \tag{13}$$

The update law $(\hat{d}_i)$ of FTDO is obtained as follows:

$$\hat{d}_i = H_{i1}\mathrm{sig}^{\delta_{i1}}(\omega_i) + H_{i2}\int \mathrm{sig}^{\delta_{i2}}(\omega_i)\mathrm{d}t, \tag{14}$$

where $H_{i1} \in \mathbf{R}^{3\times3}$ and $H_{i2} \in \mathbf{R}^{3\times3}$ are positive define diagonal matrices. $\delta_{i1} > 0$ and $\delta_{i2} > 0$ are positive constants and satisfy $0.5 \le \delta_{i1} < 1$ and $\delta_{i2} = 2\delta_{i1} - 1$, respectively.

Define the estimation error of disturbances $\tilde{d}_i = d_i - \hat{d}_i$. The time derivative of (13) is given as follows:

$$\dot{\omega}_i = d_i - \hat{d}_i = \tilde{d}_i = -H_{i1}\mathrm{sig}^{\delta_{i1}}(\omega_i) - H_{i2}\int \mathrm{sig}^{\delta_{i2}}(\omega_i)\mathrm{d}t + d_i. \tag{15}$$

Define a new variable vector $\rho_i = [x_{i1}^T, x_{i2}^T]^T = [\omega_i^T, \varsigma_i^T]^T$, where $\varsigma_i = -H_{i2}\int \mathrm{sig}^{\delta_{i2}}(\omega_i)\mathrm{d}t + d_i$. Thus, the formula (15) is rewritten as follows:

$$\dot{x}_{i1} = -H_{i1}\mathrm{sig}^{\delta_{i1}}(x_{i1}) + x_{i2}, \tag{16}$$

$$\dot{x}_{i2} = -H_{i2}\mathrm{sig}^{\delta_{i2}}(x_{i1}) + \dot{d}_i. \tag{17}$$

If a new closed-loop system is constructed by the formulas (16) and (17), then x_{i1} and x_{i2} can be regarded as the internal states of this closed-loop system. Under these circumstances, if $x_{i1} \longrightarrow 0$ and $x_{i2} \longrightarrow 0$ in finite time, then $\dot{x}_{i1} \longrightarrow 0$ and $\hat{d}_i = d_i$ in finite time.

Therefore, the following theorem holds.

Theorem 1. *The disturbance observer composed by the formulas (12) and (14), the unknown time-varying environmental disturbance can be estimated in finite time, and the disturbance estimation error converges to a neighborhood of the equilibrium point in finite time.*

Proof. The Lyapunov function V_i is chosen as follows:

$$V_i = \frac{1}{2}\chi_i^T P_i \chi_i, \tag{18}$$

where the vector χ_i and positive define matrix P_i are designed as follows, respectively.

$$\chi_i = \begin{bmatrix} sig^{\delta_{i1}}(x_{i1}) \\ x_{i2} \end{bmatrix},$$
$$P_i = \begin{bmatrix} \dfrac{2H_{i2}}{\delta_{i1}} + H_{i1}^2 & -H_{i1} \\ -H_{i1} & 2I_{3\times3} \end{bmatrix}. \tag{19}$$

Note that Lyapunov function V_i is continuous and differentiable everywhere except $\rho_i = \{(x_{i1}, x_{i2}) | x_{i1} = 0_{3\times1}\}$ and positive definite. Then, we get

$$\frac{1}{2}\lambda_{\min}(P_i)\|\chi_i\|^2 \le V_i \le \frac{1}{2}\lambda_{\max}(P_i)\|\chi_i\|^2, \tag{20}$$

where

$$\|\chi_i\|^2 = \left(sig^{\delta_{i1}}(x_{i1})\right)^2 + x_{i2}^T x_{i2} = |x_{i1}|^{2\delta_{i1}} + x_{i2}^T x_{i2}. \tag{21}$$

The time derivative of Lyapunov function V_i is given as follows:

$$\begin{aligned}
\dot{V}_i &= \chi_i^T \begin{bmatrix} \delta_{i1}H_{i1} & -H_{i2} \\ -\delta_{i1} & 0 \end{bmatrix} P_i\chi_i + \frac{1}{2}\chi_i^T P_i \begin{bmatrix} 0_{3\times3} \\ \dot{d}_i \end{bmatrix} + \chi_i^T P_i \begin{bmatrix} \delta_{i1}|x_{i1}|^{\delta_{i1}-1}\left(-H_{i1}sig^{\delta_{i1}}(x_{i1}) + x_{i2}\right) \\ -H_{i2}sig^{\delta_{i2}}(x_{i1}) \end{bmatrix} + \frac{1}{2}\chi_i^T P_i \begin{bmatrix} 0_{3\times3} \\ \dot{d}_i \end{bmatrix} \\
&= \chi_i^T P_i \begin{bmatrix} |x_{i1}|^{\delta_{i1}-1}\delta_{i1}\left(-H_{i1}sig^{\delta_{i1}}(x_{i1}) + x_{i2}\right) \\ -H_{i2}sig^{\delta_{i1}-1}(x_{i1})sig^{\delta_{i1}}(x_{i1}) \end{bmatrix} + \chi_i^T \begin{bmatrix} \delta_{i1}H_{i1} & -H_{i2} \\ -\delta_{i1} & 0 \end{bmatrix} P_i\chi_i + \chi_i^T P_i \begin{bmatrix} 0_{3\times3} \\ \dot{d}_i \end{bmatrix} \\
&= -|x_{i1}|^{\delta_{i1}-1}\chi_i^T L_i \chi_i + \chi_i^T l_i \dot{d}_i \le -\lambda_{\min}(L_i)|x_{i1}|^{\delta_{i1}-1}\|\chi_i\|^2 + c_3\|\chi_i\|\|l_i\|,
\end{aligned} \tag{22}$$

where

$$L_i = H_{i1}\begin{bmatrix} H_{i2} + \delta_{i1}H_{i1}^2 & -\delta_{i1}H_{i1} \\ -\delta_{i1}H_{i1} & \delta_{i1}I_{3\times 3} \end{bmatrix}, \quad l_i = \begin{bmatrix} -H_{i1} \\ 2I_{3\times 3} \end{bmatrix}. \tag{23}$$

From formula (21), the following inequality holds:

$$\begin{aligned} \|\chi_i\|^2 &= |x_{i1}|^{2\delta_{i1}} + x_{i2}^T x_{i2} \\ &\Rightarrow \|\chi_i\|^2 \geq |x_{i1}|^{2\delta_{i1}} \\ &\Rightarrow |x_{i1}|^{\delta_{i1}-1} \geq \|\chi_i\|^{(\delta_{i1}-1)/\delta_{i1}}. \end{aligned} \tag{24}$$

Substituting the formula (24) into (22), the inequation (22) is written as follows:

$$\dot{V}_i \leq -c_{i1}\|\chi_i\|^{\delta_{i1}+\delta_{i2}/\delta_{i1}}, \tag{25}$$

where $c_{i1} = \lambda_{\min}(L_i) - (c_3 \|l_i\|/\|\chi_i\|^{\delta_{i2}/\delta_{i1}}) = \lambda_{\min}(L_i) - c_3\|l_i\|\|\chi_i\|^{-(\delta_{i2}/\delta_{i1})}$.

To ensure the coefficient $c_{i1} > 0$, the following inequality is holds

$$\|\chi_i\| > \left(\frac{c_3\|l_i\|}{\lambda_{\min}(L_i)}\right)^{\delta_{i1}/\delta_{i2}}. \tag{26}$$

From formulas (20) and (26), the term $\dot{V}_i$ is bounded, i.e.,

$$\dot{V}_i \leq -c_{i2}V_i^{c_{i3}}, \tag{27}$$

where

$$\begin{aligned} c_{i2} &= 2c_{i1}\frac{\lambda_{\min}^{-(\delta_{i2}/2\delta_{i1})}(P_i)}{\sqrt{\lambda_{\min}(P_i)}} = 2c_{i1}\lambda_{\min}^{-c_{i3}}(P_i) > 0, \\ 0 < c_{i3} &= \frac{\delta_{i1}+\delta_{i2}}{2\delta_{i1}} < 1. \end{aligned} \tag{28}$$

According to the Lemma 1, the new closed-loop system composed of formulas (16) and (17) converges to a neighborhood of the equilibrium point in finite time.

This completes the proof.

4. Output Feedback Controller Design

In this chapter, inspired by references [29, 30], the output feedback controller is designed. The structure diagram of multiple unmanned surface vehicles swarm control is shown in Figure 2.

4.1. Auxiliary Dynamic System Design. In this subsection, the auxiliary dynamic system (ADS) is introduced to settle the input saturation problem [22]. For ADS, as shown in Figure 2, the input of the system is the difference value $(\Delta\tau_i)$ between the control forces and moments with saturation (τ_i) and those without saturation constraint (τ_{ic}). The output of ADS is the compensation of position and heading tracking error (β_{i1}) and the compensation of velocity tracking error (β_{i2}) for i th USV. The purpose of designing ADS is to compensate for the specified variables in the closed-loop system.

Among them, β_{i1} and β_{i2} are position and heading compensation and velocity compensation for z_{i1} and z_{i2}, respectively. The ADS is designed as follows:

$$\dot{\beta}_{i1} = -L_{i1}\beta_{i1} + a_{id}J_i\beta_{i2}, \tag{29}$$

$$\dot{\beta}_{i2} = -L_{i2}\beta_{i2} + M_i^{-1}\Delta\tau_i. \tag{30}$$

where $\beta_{i1} \in \mathbf{R}^{3\times 1}$ and $\beta_{i2} \in \mathbf{R}^{3\times 1}$ are the output states of the ADS. $L_{i1} \in \mathbf{R}^{3\times 3}$ and $L_{i2} \in \mathbf{R}^{3\times 3}$ are diagonal positive matrices. $a_{id} = d_i + a_{i0}$. $\Delta\tau_i = \tau_i - \tau_{ic}$, $\|\Delta\tau_i\| \leq \Delta\tau_{i,\max}$, $\Delta\tau_{i,\max} > 0$ is a positive constant.

4.2. Output Feedback Controller Design. In this subsection, the output feedback controller of multiple USVs is designed by using dynamic surface control technology [20]. The design process of output feedback controller is divided into the following steps.

Step 1. The first tracking error of the i th USV in earth-fixed frame is defined as follows:

$$z_{i1} = \sum_{j\in\mathcal{N}_i} a_{ij}\left(\eta_i - \mu_i - \left(\eta_j - \mu_j\right)\right) + a_{i0}(\eta_i - \eta_d - \mu_i) - \beta_{i1}, \tag{31}$$

where $\mathcal{N}_i$, a_{ij} and a_{i0} are defined in Section 2.2. η_i, μ_i and η_d are explained in formula (8), η_j and μ_j have similar definitions.

The time derivative of z_{i1}, and using the formula (4) and (29), we obtain as follows:

$$\begin{aligned} \dot{z}_{i1} &= \sum_{j\in\mathcal{N}_i} a_{ij}\dot{\eta}_i - \sum_{j\in\mathcal{N}_i} a_{ij}\dot{\eta}_j + a_{i0}\dot{\eta}_i - a_{i0}\dot{\eta}_d - \dot{\beta}_{i1} \\ &= \left(\sum_{j\in\mathcal{N}_i} a_{ij} + a_{i0}\right)R_i v_i - \sum_{j\in\mathcal{N}_i} a_{ij}\dot{\eta}_j - a_{i0}\dot{\eta}_d + L_{i1}\beta_{i1} - a_{id}J_i\beta_{i2} \\ &= a_{id}R_i v_i - \sum_{j\in\mathcal{N}_i} a_{ij}\dot{\eta}_j - a_{i0}\dot{\eta}_d + L_{i1}\beta_{i1} - a_{id}J_i\beta_{i2}. \end{aligned} \tag{32}$$

Choosing v_i as a virtual input in formula (32), by using dynamic surface control technology, the kinematic control law α_i is designed as follows:

$$\alpha_i = \frac{R_i^T}{a_{id}}\left\{-K_{i1}z_{i1} + \sum_{j\in\mathcal{N}_i} a_{ij}\dot{\eta}_j + a_{i0}\dot{\eta}_d - L_{i1}\beta_{i1}\right\}, \tag{33}$$

where $K_{i1} \in \mathbf{R}^{3\times 3}$ is the positive definite diagonal matrix.

From the kinematic control law obtained, it can be found that it is complex to calculate the time derivative of the α_i. Therefore, a first-order low-poss filter is introduced to settle the matter.

Let α_i pass through a first-order low-poss filter

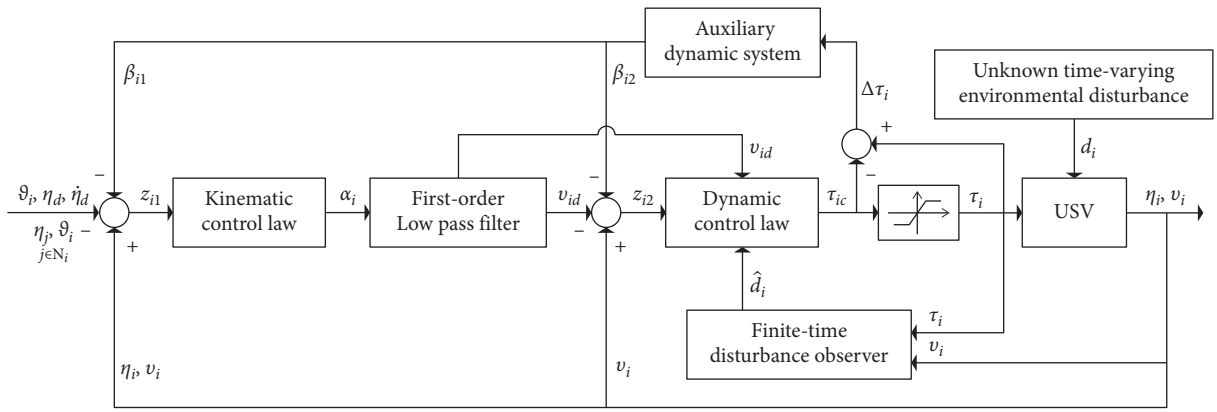

Figure 2: Structure diagram of multiple unmanned surface vehicles swarm control.

$$\begin{aligned} \iota_i \dot{v}_{id} &= \dot{\alpha}_i - v_{id}, \\ v_{id}(0) &= \alpha_i(0), \end{aligned} \tag{34}$$

where $\iota_i > 0$ is a time constant, $v_{id} \in \mathbf{R}^{3\times 1}$ is the output vector of the first-order low-poss filter.

Step 2. According to the velocity (v_i) of the i th USV, the output (v_{id}) of the first-order low-pass filter, and the state β_{i2} of ADS, the second tracking error of the i th USV is defined as follows:

$$z_{i2} = v_i - v_{id} - \beta_{i2}. \tag{35}$$

By differentiating z_{i2} and using the formula (5) and (30), we get the formula as follows:

$$M_i \dot{z}_{i2} = -D_i v_i + \tau_{ic} + d_i - M_i(\dot{v}_{id} - L_{i2}\beta_{i2}). \tag{36}$$

Furthermore, the term d_i in formula (36) is replaced by the estimated value $\widehat{d}_i$ of unknown time-varying environmental disturbance produced via the FTDO. Then, by using dynamic surface control method, the dynamic control law τ_{ic} is designed as follows:

$$\tau_{ic} = -K_{i2} z_{i2} + D_i v_i + M_i(\dot{v}_{id} - L_{i2}\beta_{i2}) - \widehat{d}_i, \tag{37}$$

where $K_{i2} \in \mathbf{R}^{3\times 3}$ is the positive definite diagonal matrix.

By substituting formula (33) and (37) into (31) and (35), the error subsystem of the i th USV is obtained as follows:

$$\dot{z}_{i1} = -K_{i1} z_{i1} + a_{id} R_i(z_{i2} + q_i), \tag{38}$$

$$M_i \dot{z}_{i2} = -K_{i2} z_{i2} - \widetilde{d}_i, \tag{39}$$

where $q_i = v_{id} - \alpha_i$, $\widetilde{d}_i$ is explained in formula (15).

According to the definition of vector q_i, by differentiating q_i, and using the formula (34), we get the equation as follows:

$$\dot{q}_i = -\frac{q_i}{\iota_i} - \dot{\alpha}_i. \tag{40}$$

By integrating the two sides of formula (40), we have the following formula:

$$q_i(t) = q_i(0) e^{-(t/\iota_i)} - \int_0^t e^{-((t-\tau)/\iota_i)} \dot{\alpha}_i(v)\mathrm{d}v. \tag{41}$$

Further calculation, the following inequality holds:

$$\begin{aligned} \|q_i(t)\| &\le \|q_i(0)\| e^{-(t/\iota_i)} + \sup_{v\in[0,t]}\{\dot{\alpha}_i(v)\} \int_0^t e^{-(t-v/\iota_i)}\mathrm{d}v \\ &\le \|q_i(0)\| e^{-(t/\iota_i)} + \iota_i \|\dot{\alpha}_i\|_\infty. \end{aligned} \tag{42}$$

Owing to the control input of adjacent USVs are bounded, i.e., $\exists \alpha_{i,\max} > 0$: $\|\dot{\alpha}_i\| \le \alpha_{i,\max}$, $\forall t \in [0, \infty]$. In fact, since all systems are energy consuming system, the output of all USVs is bounded. Therefore, the following inequality holds:

$$\|q_i(t)\| \le \|q_i(0)\| e^{-(t/\iota_i)} + \iota_i \alpha_{i,\max}. \tag{43}$$

Therefore, $q_i(t)$ is bounded and $\|q_i(t)\| \le q_{i,\max}$.

4.3. Stability Analysis

Theorem 2. *A close-loop system is considered, which is composed of n USVs cluster with input saturation, FTDO (12) and (14) with unknown time-varying environmental disturbance, ADS (29) and (30), output feedback controller (33) and (37). The swarm control scheme guarantees that all error signals in this close-loop system are bounded, and the tracking error converges to a neighborhood of the equilibrium point in finite time.*

Proof. Consider the above closed-loop system, the Lyapunov function V is chosen as follows:

$$V = \sum_{i=1}^{n} \left\{ \frac{1}{2} z_{i1}^T z_{i1} + \frac{1}{2} z_{i2}^T M_i z_{i2} + \frac{1}{2} \beta_{i1}^T \beta_{i1} + \frac{1}{2} \beta_{i2}^T \beta_{i2} \right\}. \tag{44}$$

The time derivative of V, we obtain the following equation:

$$\dot{V} = \sum_{i=1}^{n} \left\{ z_{i1}^{\mathrm{T}} \dot{z}_{i1} + z_{i2}^{\mathrm{T}} M_i \dot{z}_{i2} + \beta_{i1}^{\mathrm{T}} \dot{\beta}_{i1} + \beta_{i2}^{\mathrm{T}} \dot{\beta}_{i2} \right\}. \tag{45}$$

From the formula (32), and using Young's inequality, we get the following equation:

$$\begin{aligned} z_{i1}^T\dot{z}_{i1} &= z_{i1}^T\left(-K_{i1}z_{i1} + a_{id}R_i\left(z_{i2}+q_i\right)\right) \\ &= -z_{i1}^TK_{i1}z_{i1} + z_{i1}^Ta_{id}R_iz_{i2} + z_{i1}^Ta_{id}R_iq_i \\ &\le -z_{i1}^TK_{i1}z_{i1} + \frac{a_{id}}{2}\|z_{i1}\|^2 + \frac{a_{id}}{2}\|z_{i2}\|^2 + \frac{a_{id}}{2}\|z_{i1}\|^2 + \frac{a_{id}}{2}\|q_i\|^2 \\ &\le -z_{i1}^TK_{i1}z_{i1} + a_{id}\|z_{i1}\|^2 + \frac{a_{id}}{2}\|z_{i2}\|^2 + \frac{a_{id}}{2}\|q_i\|^2. \end{aligned} \tag{46}$$

Similarly, the following inequalities hold:

$$\begin{aligned} z_{i2}^TM_i\dot{z}_{i2} &\le -z_{i2}^TK_{i2}z_{i2} - \frac{1}{2}\|z_{i2}\|^2 + \frac{1}{2}\|\tilde{d}_i\|^2, \\ \beta_{i1}^T\dot{\beta}_{i1} &\le -\beta_{i1}^TL_{i1}\beta_{i1} + \frac{a_{id}}{2}\|\beta_{i1}\|^2 + \frac{a_{id}}{2}\|\beta_{i2}\|^2, \\ \beta_{i2}^T\dot{\beta}_{i2} &\le -\beta_{i2}^TL_{i2}\beta_{i2} + \frac{1}{2}\left(\Delta\tau_i\right)^T\left(M_i^{-1}\right)^TM_i^{-1}\Delta\tau_i + \frac{1}{2}\|\beta_{i2}\|^2. \end{aligned} \tag{47}$$

Substituting the formulas (46) and (47) into (45), then (45) is rewritten as follows:

$$\begin{aligned} \dot{V} &\le \sum_{i=1}^{n}\left\{z_{i1}^T\dot{z}_{i1} + z_{i2}^TM_i\dot{z}_{i2} + \beta_{i1}^T\dot{\beta}_{i1} + \beta_{i2}^T\dot{\beta}_{i2}\right\}, \\ &\le \sum_{i=1}^{n}\left\{-\left(\lambda_{\min}\left(K_{i1}\right) - \alpha_{id}\right)\|z_{i1}\|^2 - \left(\lambda_{\min}\left(K_{i2}\right) - \frac{\alpha_{id}+1}{2}\right)\|z_{i2}\|^2 - \left(\lambda_{\min}\left(L_{i1}\right) - \frac{\alpha_{id}}{2}\right)\|\beta_{i1}\|^2\right. \\ &\quad \left. - \left(\lambda_{\min}\left(L_{i2}\right) - \frac{\alpha_{id}+1}{2}\right)\|\beta_{i2}\|^2 + \frac{1}{2}\|\tilde{d}_i\|^2 + \frac{a_{id}}{2}\|q_i\|^2 + \frac{1}{2}\left(M_i^{-1}\Delta\tau_i\right)^TM_i^{-1}\Delta\tau_i\right\}. \end{aligned} \tag{48}$$

From the FTDO, the term $\tilde{d}_i$ converges to zero in finite time. According to the formula (43), $\|q_i(t)\| \le q_{i,\max}$. For the i th USV, M_i is a known positive constant matrix. $\|\Delta\tau_i\| \le \Delta\tau_{i,\max}$ is defined in Section 4.1. Thus, we have the following equation:

$$c_4 = \sum_{i=1}^{n}\left\{\frac{1}{2}\|\tilde{d}_i\|^2 + \frac{a_{id}}{2}q_{i,\max}^2 + \frac{1}{2}\lambda_{\min}\left(\left(M_i^{-1}\right)^TM_i^{-1}\right)\left(\Delta\tau_{i,\max}\right)^2\right\}. \tag{49}$$

where c_4 is bounded, i.e., $0 < c_4 \le c_{4,\max}$.

To ensure the stability of the closed-loop system, the parameters K_{i1}, K_{i2}, L_{i1}, and L_{i2} should meet the following conditions:

$$\begin{cases} b_{i1} = \lambda_{\min}\left(K_{i1}\right) - \alpha_{id} > 0 \\ b_{i2} = \lambda_{\min}\left(K_{i2}\right) - \dfrac{\alpha_{id}+1}{2} > 0 \\ b_{i3} = \lambda_{\min}\left(L_{i1}\right) - \dfrac{\alpha_{id}}{2} > 0 \\ b_{i4} = \lambda_{\min}\left(L_{i2}\right) - \dfrac{\alpha_{id}+1}{2} > 0 \end{cases} \tag{50}$$

where b_{i1}, b_{i2}, b_{i3}, and b_{i4} are positive constants.

Substituting the formulas (49) and (50) into (48), then (48) is rewritten as follows:

$$\begin{aligned} \dot{V} &\le \sum_{i=1}^{n}\left\{-b_{i1}\|z_{i1}\|^2 - b_{i2}\|z_{i2}\|^2 - b_{i3}\|\beta_{i1}\|^2 - b_{i4}\|\beta_{i2}\|^2\right\} + c_{4,\max} \\ &\le -bV + c_{4,\max}. \end{aligned} \tag{51}$$

where $b = 2\min\{b_{i1}, b_{i2}, b_{i3}, b_{i4}\} > 0$.

From the formula (51), either $\|z_{i1}\| > \sqrt{c_{4,\max}/b_{i1}}$, or $\|z_{i2}\| > \sqrt{c_{4,\max}/b_{i2}}$, or $\|\beta_{i1}\| > \sqrt{c_{4,\max}/b_{i3}}$, or $\|\beta_{i1}\| > \sqrt{c_{4,\max}/b_{i3}}$, then $\dot{V} \le 0$ holds. This implies that:

$$V(t) \le \left(V(0) - \frac{c_{4,\max}}{b}\right)e^{-bt} + \frac{c_{4,\max}}{b}. \tag{52}$$

It can be concluded that all signals $(z_{i1}, z_{i2}, \beta_{i1}, \beta_{i2}, \widehat{d}_i)$ in the closed-loop system are bounded. Thus, the values of variables z_{i1} and β_{i1} are given as:

$$\|z_{i1}\| \le \sqrt{\frac{c_{4,\max}}{b}}, \tag{53}$$

$$\|\beta_{i1}\| \le \sqrt{\frac{c_{4,\max}}{b}}. \tag{54}$$

Next, it will be proved that the USV cluster can track the reference signal with the desired relative deviation.

The tracking error of the i th USV in the earth-fixed frame is defined as δ_i, it satisfies the following constraints:

$$\delta_i = \eta_i - \eta_d - \mu_i, \tag{55}$$

According to the formula (31), we obtain:

$$z_1 + \beta_1 = (\mathscr{H} \otimes I_3)\delta, \tag{56}$$

where $z_1 = [z_{11}^T, z_{21}^T, \ldots, z_{n1}^T]^T$, $\beta_1 = [\beta_{11}^T, \beta_{21}^T, \ldots, \beta_{n1}^T]^T$, and $\delta = [\delta_1^T, \delta_2^T, \ldots, \delta_n^T]^T$. $\mathscr{H}$ is defined in Section 2.2.

According to the Assumption 1 of algebraic graph theory in the Section 2.2, it can be concluded that all eigenvalues of matrix $\mathscr{H}$ have positive real parts. Furthermore, using the formulas (53) and (54), we get the following equation:

$$\|\delta\| \le \frac{\|z_1\| + \|\beta_1\|}{\lambda_{\min}(\mathscr{H})} \le \frac{2\sqrt{2c_{4,\max}}}{\lambda_{\min}(\mathscr{H})\sqrt{b}}. \quad (57)$$

According to the formulas (51) and (57), by adjusting the parameters of controller and disturbance observer, the upper bound of tracking error can be reduced and finally converges to a very small neighborhood close to zero.

This completes the proof.

5. Simulation Results

In this section, a USV swarm consisting of one virtual leader vehicle (indexed by 0) and six follower USVs (indexed by $1, 2, \ldots, 6$) is considered to demonstrate the effectiveness of the proposed control strategy. The directed communication graph is shown in Figure 3.

In simulations, the model of the surface ship Cybership II is used [31]. The time-varying environmental disturbances are modeled as first-order Markov processes [24]. The control forces and moment are limited as $\tau_{i1,\max} = -\tau_{i1,\min} = 2\text{N}$, $\tau_{i2,\max} = -\tau_{i2,\min} = 2\text{N}$ and $\tau_{i3,\max} = -\tau_{i3,\min} = 1.5\text{Nm}$. The desired reference point is set as $\eta_d = [15\text{m}, 15\text{m}, 45\text{deg}]^T$. Some parameters setting are shown in Table 2.

5.1. Performance of Proposed Control Strategy. In this subsection, the simulation results are given to verify the performance of proposed control strategy.

The parameters of environmental disturbance are selected as $T = diag\{10^{-3}, 10^{-3}, 10^{-3}\}$, $b(0) = [0, 0, 0]^T$, $E_b = \text{diag}\{10^{-5}, 10^{-5}, 10^{-5}\}$, $\vartheta_b = [0.5, 0.5, 0.5]^T$. The parameters of observer are selected as $L_{i1} = \text{diag}\{10, 10, 10\}$, $L_{i2} = \text{diag}\{10, 10, 10\}$, $\delta_{i1} = 0.75$ and $\delta_{i2} = 0.5$. The design parameters of controller are chosen as $\iota_i = 0.001$, $K_{i1} = \text{diag}\{1.2, 1.2, 1.2\}$ and $K_{i2} = \text{diag}\{0.6, 0.6, 0.6\}$.

The simulation results are shown in Figures 4–8. Figure 4 shows the trajectories of six USVs under the constraints of time-varying environmental disturbance and input saturation. It can be seen from Figure 4, the position and heading of six USVs can track the reference signal in the form of swarm motion and maintain the desired relative position with each other, although there is a deviation in the initial position of each USV. Figure 5 depicts the position and heading tracking errors of six USVs. It can be seen from the figure that the tracking errors of six USVs are convergent. Figure 6 shows the control forces and moments of six USVs with an auxiliary dynamic system. Through the analysis of Figure 6, the control inputs of six USVs are limited within the range of input constraints, and finally the constraint of input amplitude saturation is realized. Figure 7 depicts the true value of the time-varying environmental disturbance acting on the 1st USV and the estimated values obtained by methods FTDO and MDA, respectively. Figure 8 shows the disturbance error ($\tilde{d}_i$) of six USVs between the actual value (d_i) and estimation value ($\hat{d}_i$) via the FTDO. The specific values of simulation test and comparison test are shown in Table 3.

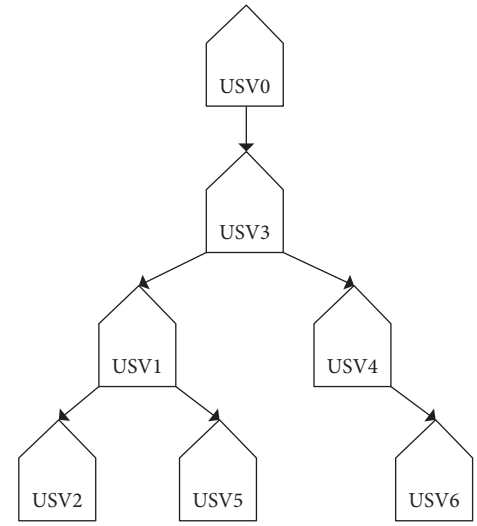

Figure 3: Directed communication topology.

Table 2: The parameters of six follower USVs.

μ_i	data/ (m, m, deg)	η_i	data/ (m, m, deg)
μ_1	$[-2.8, 0.3, 0]^T$	η_1	$[-2.5, 0, 0]^T$
μ_2	$[-1.6, 2.5, 0]^T$	η_2	$[-1.3, 2.2, 0]^T$
μ_3	$[-1.6, 1.9, 0]^T$	η_3	$[-1.3, -2.2, 0]^T$
μ_4	$[1.0, 2.5, 0]^T$	η_4	$[1.3, 2.2, 0]^T$
μ_5	$[1.6, -2.5, 0]^T$	η_5	$[1.3, -2.2, 0]^T$
μ_6	$[2.2, -0.3, 0]^T$	η_6	$[2.5, 0, 0]^T$

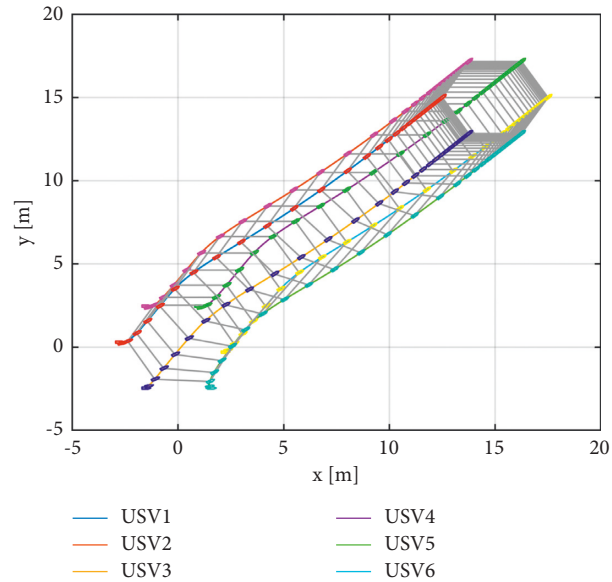

Figure 4: Trajectories of six follower USVs.

5.2. Comparison Group. The first comparison simulation is carried out by using a modular design approach (MDA) proposed in [20].

Simulation results on the proposed predictor module for estimating the value and estimation error of the unknown

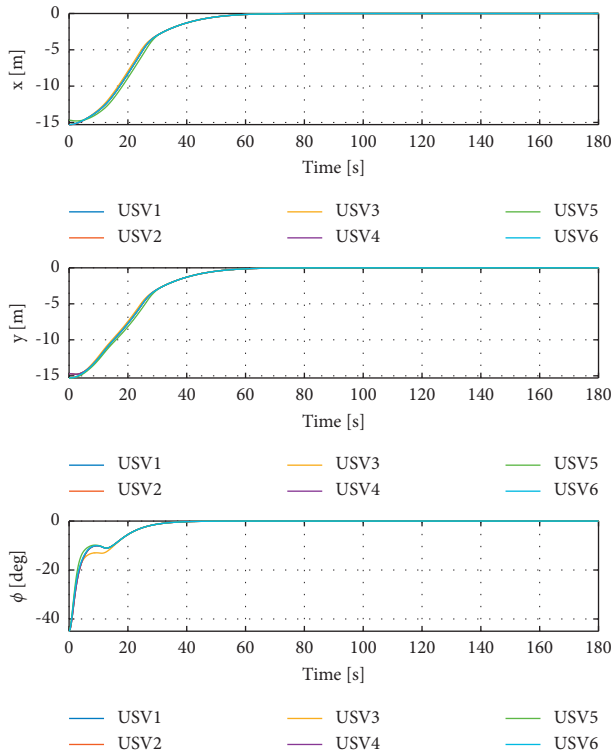

Figure 5: Tracking errors of six follower USVs.

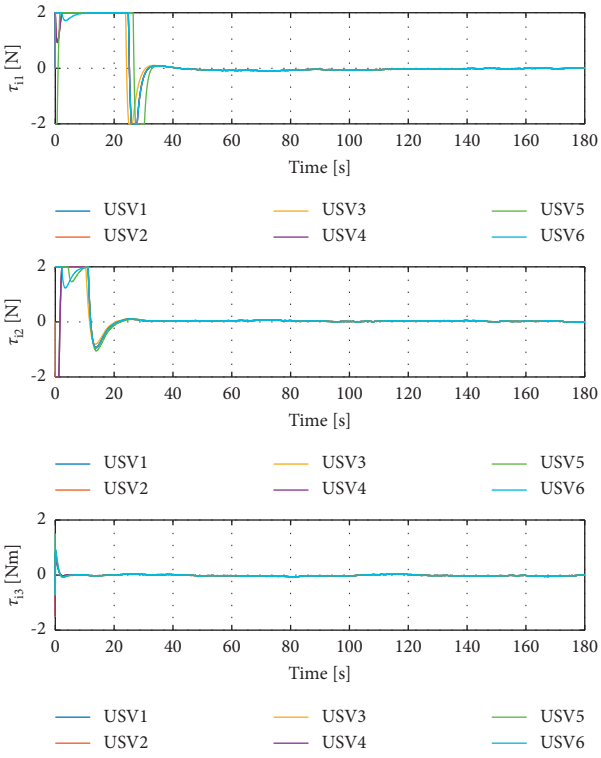

Figure 6: The control input (τ_i) of six USVs with ADS.

ocean disturbances are shown in Figures 7 and 9. Figure 7 shows the different time-varying environmental disturbance estimations of the 1st USV about actual value, MDA, and

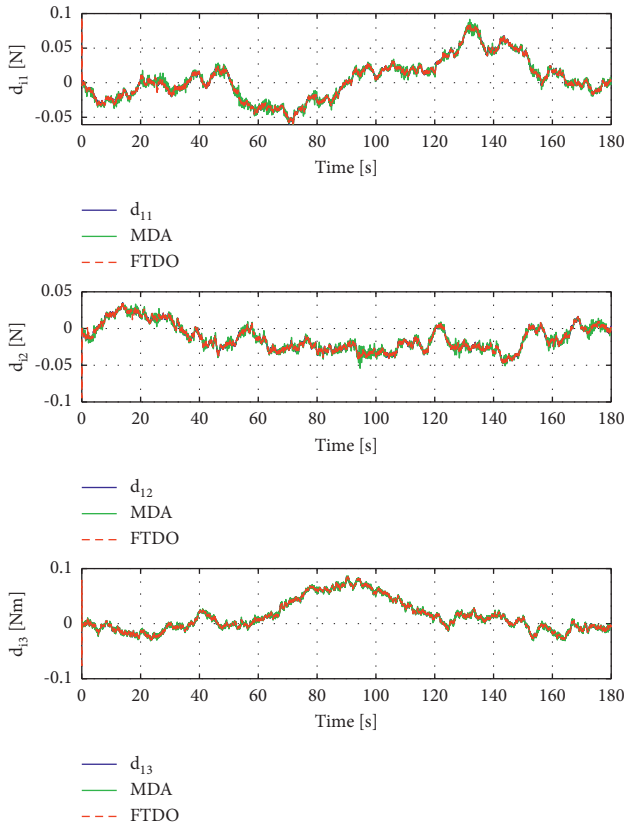

Figure 7: The time-varying environmental disturbance estimation of the 1th USV.

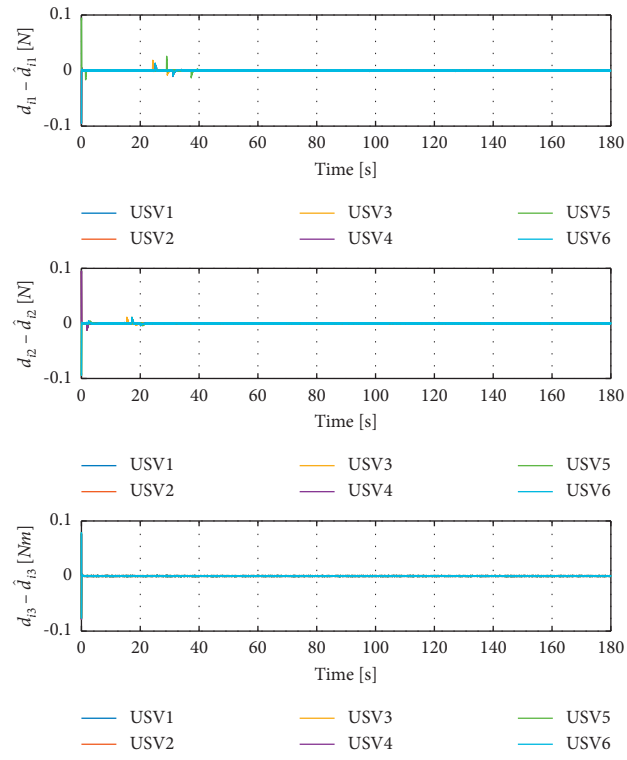

Figure 8: The disturbance error $(\tilde{d}_i)$ of six USVs.

Table 3: Specific values of simulation test and comparison test.

	Performance parameter	Values
Consider ADS	Convergence time	24.0 s
No ADS	Convergence time	31.2 s
Consider input saturation	$\tau_{i1,\max}$ and $\tau_{i2,\max}$	2 N
No input saturation	$\tau_{i1,\max}$ and $\tau_{i2,\max}$	200 N
Consider input saturation	$\tau_{i3,\max}$	1.5 Nm
No input saturation	$\tau_{i3,\max}$	150 Nm

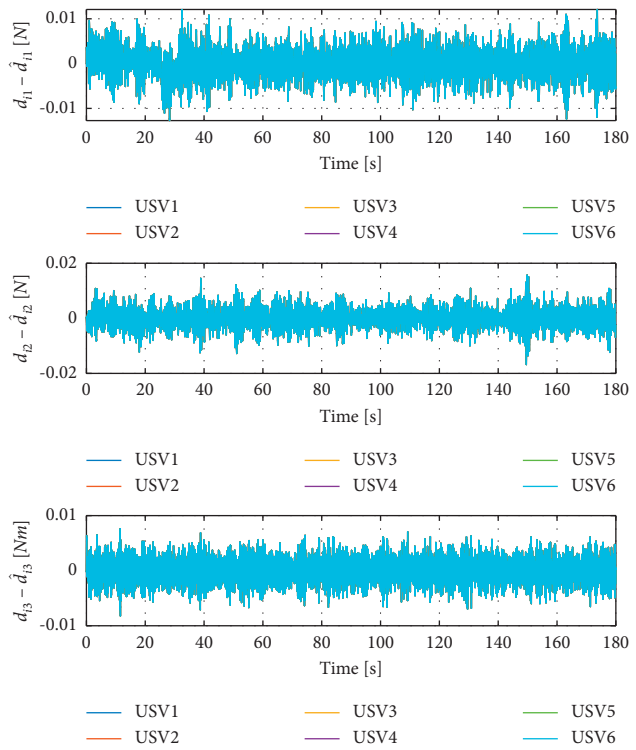

Figure 9: The disturbance error $(\tilde{d}_i)$ of six USVs via MDA.

FTDO, respectively. Figure 9 shows the disturbance error of six USVs by using MDA. From Figures 7–9, the control inputs of two methods are both limited, but the more accurate estimation of the environmental disturbance is obtained by FTDO.

The other simulation results of the proposed state feedback controller without the auxiliary dynamic system and input saturation are illustrated in Figures 10 and 11, Figure 10 shows the control input of six follower USVs without considering the auxiliary dynamic system. Figure 11 shows the control input of six follower USVs without actuator constraint. Through comparing Figures 6, 10, and 11, the auxiliary dynamic system can effectively finish off the input saturation, and it is very necessary to take the physical constraints of the system into account when designing the controller.

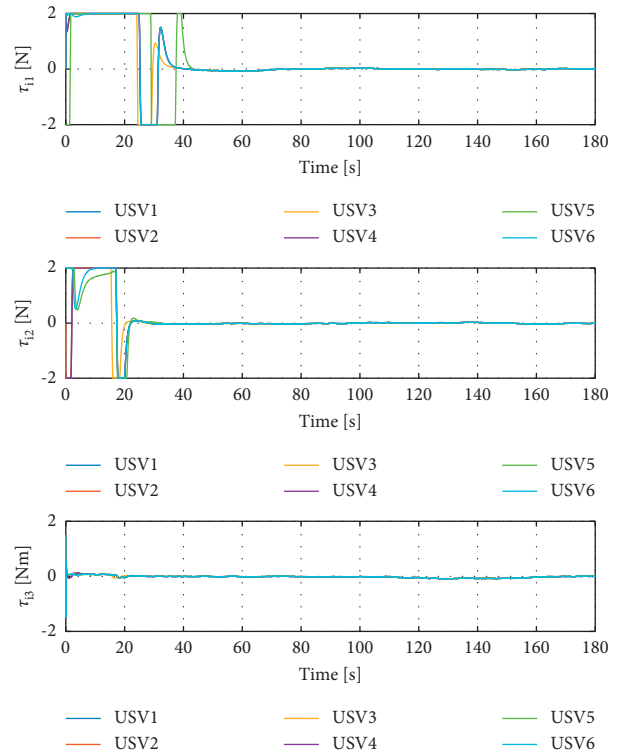

Figure 10: The control input (τ_i) of six USVs with the input saturation without ADS.

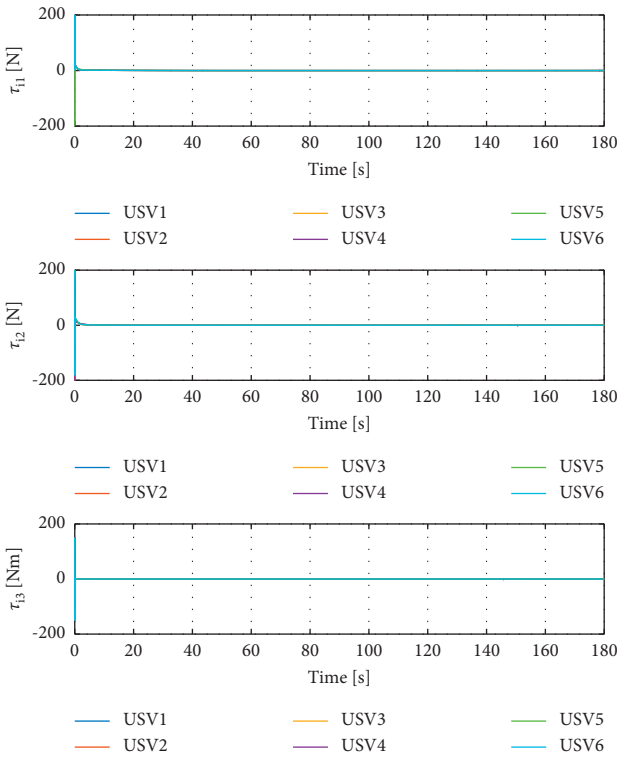

Figure 11: The control input (τ_i) of six USVs without the actuator constraint.

6. Conclusion

This paper investigates swarm control for multiple USVs in the presence of an unknown time-varying environmental disturbance and input saturation. Firstly, an observer is designed to estimate disturbance by using finite time control technology. Secondly, an auxiliary dynamic system is introduced to finish off the input saturation problem. Thirdly, an output feedback controller is designed, which is mainly composed of a finite-time disturbance observer, an auxiliary dynamic system, and other control technologies. At the same time, the stability of the system is proved by the Lyapunov method. Finally, the effectiveness of the proposed control strategy is verified by simulation results.

However, in the design process of the controller, only input amplitude saturation and time-varying environmental disturbance are considered: collision avoidance and obstacle avoidance are ignored. Safe, reliable, and collision-free track planning is an important research direction in the field of unmanned surface vehicles. This is the focus of our future research.

Data Availability

The data used to support the findings of this study are available from the corresponding author upon request.

Conflicts of Interest

The authors declare that there are no conflicts of interest.

Acknowledgments

This study is funded by the 7th Generation Ultra Deep Water Drilling Unit Innovation Project.

References

[1] Y. Wu, K. H. Low, and C. Lv, "Cooperative path planning for heterogeneous unmanned vehicles in a search-and-track mission aiming at an underwater target," *IEEE Transactions on Vehicular Technology*, vol. 69, no. 6, pp. 6782–6787, 2020.

[2] A. Macwan, J. Vilela, G. Nejat, and B. Benhabib, "A multi-robot Path-planning strategy for autonomous wilderness search and rescue," *IEEE Transactions on Cybernetics*, vol. 45, no. 9, pp. 1784–1797, 2015.

[3] P. Mahacek, C. A. Kitts, and I. Mas, "Dynamic guarding of marine assets through cluster control of automated surface vessel fleets," *IEEE*, vol. 17, no. 1, pp. 65–75, 2012.

[4] E. Raboin, P. Švec, D. S. Nau, and S. K. Gupta, "Model-predictive asset guarding by team of autonomous surface vehicles in environment with civilian boats," *Autonomous Robots*, vol. 38, no. 3, pp. 261–282, 2014.

[5] G. Xia, C. Sun, B. Zhao, X. Xia, and X. Sun, "Neuroadaptive distributed output feedback tracking control for multiple marine surface vessels with input and output constraints," *IEEE Access*, vol. 7, Article ID 123076, 2019.

[6] Y. Lu, G. Zhang, Z. Sun, and W. Zhang, "Adaptive cooperative formation control of autonomous surface vessels with uncertain dynamics and external disturbances," *Ocean Engineering*, vol. 167, pp. 36–44, 2018.

[7] X. Li, P. Shi, and Y. Wang, "Distributed cooperative adaptive tracking control for heterogeneous systems with hybrid nonlinear dynamics," *Nonlinear Dynamics*, vol. 95, no. 3, pp. 2131–2141, 2018.

[8] M. Lu, L. Liu, and G. Feng, "Adaptive tracking control of uncertain Euler-Lagrange systems subject to external disturbances," *Automatica*, vol. 104, pp. 207–219, 2019.

[9] Z. Jia, Z. Hu, and W. Zhang, "Adaptive output-feedback control with prescribed performance for trajectory tracking of underactuated surface vessels," *ISA Transactions*, vol. 95, pp. 18–26, 2019.

[10] X. Yan, Y. Liu, and W. X. Zheng, "Global adaptive output-feedback stabilization for a class of uncertain nonlinear systems with unknown growth rate and unknown output function," *Automatica*, vol. 104, pp. 173–181, 2019.

[11] J. Zhang, S. Yu, and Y. Yan, "Fixed-time output feedback trajectory tracking control of marine surface vessels subject to unknown external disturbances and uncertainties," *ISA Transactions*, vol. 93, pp. 145–155, 2019.

[12] J. Yu, P. Shi, and L. Zhao, "Finite-time command filtered backstepping control for a class of nonlinear systems," *Automatica*, vol. 92, pp. 173–180, 2018.

[13] S. P. Bhat and D. S. Bernstein, "Finite-time stability of continuous autonomous systems," *SIAM Journal on Control and Optimization*, vol. 38, no. 3, pp. 751–766, 2000.

[14] H. Yan, Y. Tian, H. Li, H. Zhang, and Z. Li, "Input-output finite-time mean square stabilization of nonlinear semi-Markovian jump systems," *Automatica*, vol. 104, pp. 82–89, 2019.

[15] Y. Sun, G. Ma, M. Liu, C. Li, and J. Liang, "Distributed finite-time coordinated control for multi-robot systems," *Transactions of the Institute of Measurement and Control*, vol. 40, no. 9, pp. 2912–2927, 2017.

[16] H. Du, G. Wen, X. Yu, S. Li, and M. Z. Q. Chen, "Finite-time consensus of multiple nonholonomic chained-form systems based on recursive distributed observer," *Automatica*, vol. 62, pp. 236–242, 2015.

[17] B. Huang, S. Song, C. Zhu, J. Li, and B. Zhou, "Finite-time distributed formation control for multiple unmanned surface vehicles with input saturation," *Ocean Engineering*, vol. 233, Article ID 109158, 2021.

[18] Q. Zhu and Y. Liu, "Neural network adaptive finite-time control of stochastic nonlinear systems with full state constraints," *Asian Journal of Control*, vol. 23, no. 4, pp. 1728–1739, 2020.

[19] G. Miao, Q. Ma, and Q. Liu, "Consensus problems for multi-agent systems with nonlinear algorithms," *Neural Computing & Applications*, vol. 27, no. 5, pp. 1327–1336, 2015.

[20] Z. Peng, D. Wang, and J. Wang, "Cooperative dynamic positioning of multiple marine offshore vessels: a modular design," *IEEE*, vol. 21, no. 3, pp. 1210–1221, 2016.

[21] X. Zhang, L. Liu, and G. Feng, "Leader-follower consensus of time-varying nonlinear multi-agent systems," *Automatica*, vol. 52, pp. 8–14, 2015.

[22] W. Zhou, Y. Wang, C. K. Ahn, J. Cheng, and C. Chen, "Adaptive fuzzy backstepping-based formation control of unmanned surface vehicles with unknown model nonlinearity and actuator saturation," *IEEE Transactions on Vehicular Technology*, vol. 69, no. 12, pp. 14749–14764, 2020.

[23] T. I. Fossen and J. P. Strand, "Passive nonlinear observer design for ships using Lyapunov methods: full-Scale experiments with a supply vessel," *Automatica*, vol. 35, no. 1, pp. 3–16, 1999.

[24] T. I. Fossen, "How to incorporate wind, waves and ocean currents in the marine craft equations of motion," *IFAC Proceedings Volumes*, vol. 45, no. 27, pp. 126–131, 2012.

[25] G. Xia, X. Shao, and A. Zhao, "Robust nonlinear observer and observer-backstepping control design for surface ships," *Asian Journal of Control*, vol. 17, no. 4, pp. 1377–1393, 2015.

[26] J. Cheng, L. Liang, H. Yan, J. Cao, S. Tang, and K. Shi, "Proportional-integral observer-based state estimation for Markov memristive neural networks with sensor saturations," *IEEE Transactions on Neural Networks and Learning Systems*, pp. 1–12, 2022.

[27] J. Cheng, L. Liang, J. H. Park, H. Yan, and K. Li, "A dynamic event-triggered approach to state estimation for switched memristive neural networks with nonhomogeneous sojourn Probabilities," *IEEE Transactions on Circuits and Systems I: Regular Papers*, vol. 68, no. 12, pp. 4924–4934, 2021.

[28] J. Cheng, Y. Wang, J. H. Park, J. Cao, and K. Shi, "Static output feedback quantized control for fuzzy markovian switching singularly Perturbed systems with deception attacks," *IEEE Transactions on Fuzzy Systems*, vol. 30, no. 4, pp. 1036–1047, 2022.

[29] G. Xia, C. Sun, B. Zhao, and J. Xue, "Cooperative control of multiple dynamic positioning vessels with input saturation based on finite-time disturbance observer," *International Journal of Control, Automation and Systems*, vol. 17, no. 2, pp. 370–379, 2019.

[30] M. R. Mokhtari, B. Cherki, and A. C. Braham, "Disturbance observer based hierarchical control of coaxial-rotor UAV," *ISA Transactions*, vol. 67, pp. 466–475, 2017.

[31] R. Skjetne, T. I. Fossen, and P. V. Kokotović, "Adaptive maneuvering, with experiments, for a model ship in a marine control laboratory," *Automatica*, vol. 41, no. 2, pp. 289–298, 2005.